Research Square

Preprints are preliminary reports that have not undergone peer review.
They should not be considered conclusive, used to inform clinical practice,
or referenced by the media as validated information.

Enzymatic Extraction and Characterization of Nanocellulose from Cornhusk Fiber

Haiyan Jin
Qiqihar University
yinghua tian (yinghua_tian@163.com)
Qiqihar University https://orcid.org/0000-0003-0447-0950
Liqian Teng
Qiqihar University
Jiaqi Yang
Qiqihar University
Hongyan Wu
Qiqihar University
Xiaolan Liu
Qiqihar University

Research Article

Keywords: cornhusk fiber, nanocellulose, enzyme extraction, particle size distribution

Posted Date: August 26th, 2022

DOI: https://doi.org/10.21203/rs.3.rs-1576975/v1

License: This work is licensed under a Creative Commons Attribution 4.0 International License.
Read Full License

Abstract

Cornhusk is a renewable and abundant crop by-product whose diverse applications must be studied more extensively. However, thus far, cornhusk, as a raw material, has not been employed for production of cornhusk fiber (CF) nanocellulose (CNC). This study aims to extract and characterize nanocellulose using CF as a raw material by high-shear-assisted enzyme hydrolysis. The extraction process was optimized by investigating the particle size distribution. The optimal extraction conditions of CNC were as follows: cellulase concentration of 1 mg/g, pH of 4.8, temperature of 50 ℃, and 24 h treatment under high-shear conditions for 20 min. The morphological characteristics of the CNC and CF were investigated, and FTIR、XRD, and TGA analyses were performed. Compared with CF, CNC exhibited slenderer nanofibrils with a smoother surface. FTIR analysis showed that the peaks that represented hemicellulose, lignin, and pectin disappeared or diminished in the CNC spectrum. The crystal type of CNC did not change and was identical to that of CF (cellulose type I). The TGA results showed that CNC possessed a lower thermal stability and higher char residuals than those of CF.

1. Introduction

As the advantages of large surface area, light weight, high strength and good biocompatibility, nanocellulose has broad application prospects. With the rapid development of natural fibers nanotechnology, there has been substantial research on developing a highly efficient and low-cost method to prepare nanocellulose (CNC). CNC is usually extracted by chemical and enzyme treatment(Reddy et al., 2005), acid hydrolysis, or mechanical methods, such as microwave(Singh et al., 2017), high-shear(Mahardika et al., 2018), ultrasonication(Wang et al., 2016), cellulolytic enzyme treatment(Kumari et al., 2019), and TEMPO oxidation(Chao Du et al.,2016). However, these methods have some drawbacks; for example, the mechanical method entails a high energy consumption, and the ideal particle size cannot be obtained by using this method alone. A small particle size can be obtained by chemical treatment and acid hydrolysis; however, the introduction of chemical substances affects the practical application of these methods. The enzymatic method does not require solvents or acidic reagents, entails mild conditions, and affords a relatively high yield. Hence, it is considered that enzyme is suitable for isolating CNC from natural fibers(Henriksson et al., 2007).

Natural fibers are cost-efficient, environment friendly, and source abundant. Cornhusk fiber (CF), which is extracted from cornhusk by using physical, chemical, and biological methods(Reddy et al., 2005), is an example of a potentially renewable, low-cost, and sustainable natural fiber. CF possesses good mechanical properties, such as moderate elasticity and strength, and its cellulose content is high, making it an optimal material for CNC extraction. Recently, cellulose nanocrystals, nanofibers, CNCs, crystallites and other nanoscale cellulose materials have attracted increasing interest owing to their biocompatibility, biodegradability, renewability, sustainability, adaptable surface chemistry and other advantageous characteristics (Lagerwall et al., 2014; Trache et al.,2017). Additionally, nanoscale materials have been used in several applications, such as in barrier films(Faradilla et al., 2017), pharmaceuticals, slow drug

release(Ullah et al., 2016), paper(Liangbing Hu et al., 2013), photonics(Natarajan et al., 2018), and separation membranes(Henrique et al., 2013).

It is very important to extract the source code of NC, because it determines the size and nature of the NC provided. (Kargarzadeh et al., 2017). In the past ten years, agricultural wastes or by-products have been investigated as sources for NC extraction., for example cotton stalks(Kargarzadeh et al., 2017; Rahbar Shamskar et al., 2016), walnut shells(Hemmati et al., 2018), wheat straws, flax fibers(W. Chen et al., 2011), pineapple peels(Dai et al., 2018), corncobs(Ditzel et al., 2017), soy hulls(Flauzino Neto et al., 2013), banana peels(Khawas et al., 2016), oil palm biomass(Haafiz et al., 2014), sugarcane bagasse(Mandal et al., 2011), red algae marine biomass(Y. W. Chen et al., 2016), and sugar beet pulp(Li et al., 2014), Notably, the sustainability of corn production would significantly increase by the extraction of CNC from CF. Furthermore, global corn production in 2018–2019 was about 1.1 billion tons, and a large amount of cornhusk waste is difficult to treat and digest, it would provide terms of settlement to many of problems related to cornhusk recycle and could generate an additional source of income for farmers.

Microfibers are composed of crystalline and amorphous segments, which are repeated and interwoven. Chemical treatment can dissolve the amorphous region of CF, yielding CNC. Mendes *et al.* isolated nanocrystalline cellulose from cornhusk using H_2SO_4 hydrolysis(Carlos Augusto de Carvalho Mendes et al., 2015). As the reaction time increased, the crystallinity index and particle size of cellulose were affected, and the thermal stability decreased. Nanocellulose prepared by the TEMPO oxidation of cornhusk did not destroy the original type (□type) and structure of cellulose, but increased its crystallinity and weakened its thermal stability. Notably, cornhusk has not yet been widely studied as a raw material for producing CNC.

Herein, the extraction of CNC from CF using the enzymatic method under high shear is investigated. The characterization of this transformation was performed by morphology studies, FTIR, X-ray diffraction, and TGA. Furthermore, the effects of the enzymatic treatment on the CNC were studied based on the particle size distribution.

2. Materials And Methods

2.1 Materials

Cornhusk was collected from a corn in Hei Long Jiang Province, China. Laccase and pectinase were purchased from DENYKEM Biotechnology Co., Ltd., Shanghai, China. Xylanase was purchased from Sukahan Biological Engineering Co., Ltd., Shandong, China. Cellulase from Trichoderma viride was provided by Yuanye Biotechnology Co., Ltd., Shanghai, China. Sodium hydroxide (NaOH) and glacial acetic acid (HAC) were purchased from Kaitong Chemical Reagent Co., Ltd., Tianjin, China. Sodium acetate (NaAC) was supplied by Komil Chemical Reagents Co., Ltd., Tianjin, China. All chemical reagents are analytically pure.

2.2 Preparation of CF from cornhusk

CF was soaked for 72 h in a mixed enzyme fluid that included laccase, pectinase, and xylanase (liquor ratio 1:50, pH 4.6). The concentrations of laccase, pectinase, and xylanase were 1g/L, 3 g/L, and 2 g/L, respectively. Then, CF was washed with water to remove pectin complex and dried at 75 ℃ for 24 h. Finally, CF was ground by a grinder and sieved using a 60-mesh sieve.

2.3 Preparation of CNC from CF

Sieved fibers (1 g) were swelled using 10 mL of NaOH (0.2 mol/L) at 50 ℃ for 24 h, and the pH of the suspension was restructured to 4.8 by HAc. Then, the NaAC-HAC buffer, whose pH was 4.8, was added until the volume of the suspension was 20 mL. Low-speed shearing was used to remove foam. After the shearing ended, 10 mL of the NaAC-HAC buffer and 1 mg of cellulase were added. The mixture was cultivated in a shaker at 50 ℃ for 24 h. At the end of the enzyme treatment, the suspension was homogenized by stirring at 10000 rpm at 18–25℃ for 20 min. Finally, the treated suspension was filtered, and the filtrate was lyophilized into CNC particles.

2.4 Particle Size Analysis

The particle size distribution analysis of the samples was carried out by using a particle size analyzer (NANO. ZS90, MALVERN, UK). The filtrate was collected by vacuum filtration from the suspension, which was diluted to a concentration of 1g/L before to analysis.

2.5 Morphology analysis

The surface morphology of the CF and CNC was observed using a SEM (Model: Hitachi S-3400) under 10 kV accelerating voltage. All samples were dried until constant weight prior to investigation.

2.5 FTIR spectra

The chemical functional groups of the cornhusk, CF, and CNC were analyzed by FTIR. The pellet was made by mixing 5.0 mg of the powdered samples and 200 mg of KBr and pressing it into a disk. FTIR spectra were recorded in the wavenumber range of 500 cm^{-1} to 4000 cm^{-1}.

2.6 Crystallinity Analysis

X-ray diffraction (Bruker-AXS-D8, Germany) was used to determine crystallinity of the cornhusk, CNC, and CF at different stages of the treatments. The samples were irradiated with Cu Kα radiation in the 2θ range of 10° to 60°. The crystallinity index (CI) of cornhusk, CF, and CNC were calculate using the diffraction peak intensity method.

$$CI(\%) = (I_{002} - I_{amp} / I_{002} \times 100\%$$

1

where CI is the crystallinity index, I_{002} is the maximum intensity of the diffraction from the 002 plane, and I_{amp} is the intensity scattered by the amorphous part of the sample.

2.7 TGA Analysis

The thermal stability of the sample was determined by TGA analysis using the thermogravimetric analyzer SDT-Q600, NETZSCH (Germany). Specifically, 5 mg of the powdered samples were analyzed under N_2 flow at a rate of 20 mL/min, temperature range of 25–600 ℃, and heating rate of 20°C/min.

3. Results And Discussion

3.1 Extraction of CNC

3.1.1 Effect of enzyme concentration on CNC

Cellulose is a polymer ($(C_6H_{10}O_5)_n$) linked by β-(1,4) glucosidic bonds linked irregular network polymer. The cellullase in our experiment is a multicomponent enzyme system that includes endoglucanase (EGs) and cellobiohydrolase (CBH). EG acts on the amorphous region inside the cellulose polysaccharide chain; it randomly hydrolyzes β-(1,4)-glycosidic bonds to trounce fibrous molecules from the interior of long chains to form small fibrins. CBH mainly acts on the surface of the crystalline and amorphous zones of cellulose by acting on the linear ends of cellulose molecules. The cellulase concentration was adjusted to 1 mg/g, 3 mg/g, and 5 mg/g, with a treatment time of 24 h. Figure 1 reflects the correlation between enzyme concentration and the CNC particle size. CNC exhibits a broader size distribution and decreased signal intensity with an increase in the dose of cellulase. The particle size distribution is relatively narrow when the cellulase concentration is 1 mg/g. When the concentration of cellulase is increased from 1 mg/g to 3 mg/g and 5 mg/g, peaks with intensities of 18.4, 13.9 and 15.1 are observed, respectively. This behavior is likely result from the break down of long chains of cellulose, which gives rise to CNC with large particle sizes. Furthermore, the smaller CNC particle size probably originates from the further decomposition of CNC into polysaccharides.

3.1.2 Effect of time on extracted CNC

As the enzyme treatment efficiency is influenced by treated time, the extraction process of CNC was carried out for 12 h, 24 h, 48 h, and 72 h. The particle size distribution changes with the extraction time shown in Fig. 2. The broadest distribution and lowest intensity are exhibited when the treatment time is 12 h. When the time increases to 24 h, the intensity of the particle size peak reaches 18.4. As the treatment time is extended, the CNC particle size distribution begins to broaden slightly and intensity presents to decrease. This may be because easily degradable and short-chain cellulose is gradually hydrolyzed to form particles with smaller sizes at an early stage. Such particles of CNC are further hydrolyzed by enzymes into soluble oligosaccharides and monosaccharides, while the longer cellulose chains are degraded into large cellulose particles, causing the evolution of particle size from large to small and then to large.

3.1.3 Effect of temperature on extracted CNC

Temperature is a factor that influences diffusion and enzyme activity. An appropriate temperature can improve the efficiency of the enzymatic reaction, resulting in the efficient degradation of CF to produce

CNC. The particle size distribution of CNC extracted at different temperatures (30 ℃, 40 ℃, 50 ℃, and 60 ℃) is shown in Fig. 3. With an increase in treatment temperature from 30 ℃ to 50 ℃, the intensity of the CNC particle size peak reaches 18.4. As the treatment temperature is increased to 60 ℃, a broader size distribution and lower intensity are exhibited. with the treatment temperature increased, the enzyme activity may be increased in the lower temperature range, which promoted the hydrolyzation of the long-chain cellulose to small cellulose particles. However, when the treatment temperature is 60 ℃, the high temperature damages the cellulase protein structure, decreasing the enzyme activity and resulting in a smaller particle size peak and broader particle size distribution.

3.1.4 Effect of pH on extracted CNC

The change of pH could affect the degree of dissociation of the necessary groups on the enzyme active centerand the degree of dissociation of the substrate and the coenzyme, thereby affecting the extraction of CNC from CF and the particle size distribution of CNC. Figure 4 showed the effect of pH on CNC extraction using cellulase. The pH was adjusted from 3.2 to 5.6 by the NaAC-HAC buffer in the experiment. A narrower size distribution and higher intensity is exhibited at pH 4.8, and the intensity of CNC is reached about 18.4. The half width of particle size distribution of CNC at pH 4.8 is narrower than other pH size distributions. It may be concluded that the binding of cellulase to a substrate reached the optimum state and the catalytic reaction efficiency of CF degradation to CNC was improved at pH 4.8.

3.2 Characterization of CNC properties

3.2.1 Morphology analysis

The morphological characteristics of CNC are affected by different treatment methods and raw materials. Figure 5 shows SEM images of the surface morphology of CF and CNC. CF particles are large and the surface is rough, which may be caused by the adhesion of non cellulosic substances on the surface. By contrast, CNC has a net-like structure with slender nanofibrils. The lignin and hemicellulose were removed from the internal structure of the cellulose due to the effective action of cellulase and alkali on the amorphous region. As a result, CNC presented a cleaner and smoother surface. Further, a partial cellulose aggregation structure is clearly observed, which might be resulted of the breaking of hydrogen bonds by cellulase treatment and their rejoining by lyophilization when the dispersing medium is removed.

3.2.2 FTIR spectra

Using FTIR spectra to understand the transformation of chemical functional groups present in the studied materials. Figure 6 presents the FTIR spectra of CF (a) and CNC (b). All spectra showed typical absorption peaks of the lignocellulosic components. The broadband absorbance peaks of all samples around 3420 cm^{-1} and 2920 cm^{-1} were attributed to stretching vibrations of the hydroxyl (OH) and C–H (Chirayil et al., 2014). The peaks around 1637 cm^{-1} were put down to the O-H bending in absorbed water(Mohaiyiddin et al., 2016). The peak around 1733 cm^{-1} corresponded to the C = O stretching vibration of the acetyl and/or ketone groups of hemicellulose or carboxyl groups of lignin(Yang, et al., 2017). The small shoulder peaks at 1257 cm^{-1}, 1513 cm^{-1}, and 830 cm^{-1} were put down to C-H out-of-plane stretching vibrations,

aromatic skeletal vibrations, and aromatic C-H out-of-plane bending vibrations in lignin respectively (Islam et al., 2011). The three peaks at 1257 cm^{-1}, 1513 cm^{-1}, and 830 cm^{-1} almost disappeared in the spectrum of CNC(a) but are present in the CF one (b), which proved that cellulose was effectively dissociated from the network of lignin and hemicellulose. The peak around 1048 cm^{-1} were put down to the C-O stretching vibration of cellulose; this peak was sharper in the spectrum of CNC than in that of CF, which indicates that non-cellulosic parts were removed from the natural fiber during the enzyme treatment and the major content of the CNC is cellulose. In addition, the peaks around 1637 cm^{-1} and 1376 cm^{-1} were due to the O-H bending corresponding to the absorbed water in cellulose, intermolecular hydrogen attraction at C_6 group and C-H bending vibration of cellulose(Haafiz et al., 2014). The above absorption peaks became weak, may be indicate that water-absorbing quality of prepared CNC would decrease.

3.2.3 Crystallinity

Cellulose is composed of crystalline and amorphous regions, which affect the mechanical and thermal properties of materials (Johar et al., 2012). Figure 7 illustrates the XRD spectra of CF (a) and CNC (b). All the samples have strong diffraction peaks at 2θ = 16° (plane (101)) and 2θ = 22° (plane (002)), which is indicative of type I cellulose. The peak of CNC decreases at 2θ = 34.6 (plane (040)); this may be because enzyme treatment destroyed the crystal structure of cellulose, which also corroborates the FTIR spectra analysis.

The CI of CF and CNC, calculated by Eq. 1, is 43.17% and 35.73%, respectively. Compared with that of CF, the CI of CNC is 17.23% lower. The change of CI in this research is similar to the results of *Suqin Luo* and *Xia Li* (Suqin Luo et al., 2018; Xia Li et al., 2012). This might be attributed to the enzymatic hydrolysis process, as cellulase has a strong effect on the CF and crystalline zones may be destroyed. The change in crystal structure of cellulose increased the enzyme acting sit and varied the spacing between crystal faces and positions of active hydroxyl groups, thereby accelerating cellulose degradation(Ishikawa et al., 1997).

3.2.4 TGA Analysis

The thermal stability of CF (a) and CNC (b) was study by TGA Analysisused to, as shown in Fig. 8. Thermal degradation of the samples occurred in different stages because of different components of the sample (Sun et al., 2000). The degradation temperatures of CNC are clearly lower than those of CF. Additionally, in all the TGA and DTG curves, the initial mass reduction, result of the volatilization of bound water and volatile materials present in the samples, occurs at relatively low temperatures. The weight loss of CNC at this stage was higher than that of CF, which might be attributed to cellulose moisture absorption. The corresponding part of the DTG curve displayes a small trough around 70–100 ℃ for the same reason. For the CF, the DTG curves showed two decomposition steps, at 240 ℃-370 ℃ and 370 ℃-400 ℃. The first weight loss stage of CF at 240 ℃-370 ℃, corresponding to a mass loss of 61.73%, was attributed to the severe decomposition of hemicellulose or pectin(Xiao et al., 2016), as a part of the fiber is broken down and lost as CO_2 and volatile hydrocarbons during the pyrolysis process(Asrofi et al.,

2018). The next weight loss stage of CF at 370 ℃-400 ℃ corresponded to a mass loss of 11.40%, which is attributed to lignin pyrolysis. The solid residues of CF accounted for the 13.92% mass loss at 600°C.

The highest weight loss stage of CNC was observed at 150℃-350℃ in the DTG curve, corresponding to a mass loss of 53.43% related to the irreversible degradation of cellulose (Liu et al., 2014). From the TGA and DTG curves, the degradation temperature of CF was lower than that of CNC, which showed that the thermal stability of CNC was lower than CF. There are two reasons that can explain the lower thermal stability of CNC. First, CNC has a smaller particle size and loose cellulose structure, which is consistent with the results of SEM analysis. Its higher specific surface area and CNC surface active groups reduce its thermal stability. Second, during the enzymatic degradation of CF to CNC, cellulose chain segments are damaged and fractured(Yang et al., 2017), creating low molecular weight chains and breaking points in the structure of cellulose that lead to the reduction of thermal stability of CNC (Yang et al., 2017). Furthermore, the mass of the char residue of CNC at 600 ℃ was 26.26%, which was higher than that of CF. This might be because the dehydration and cross-linking reactions of CNC at low temperatures cause the carbonization of the cellulose polymer, this is identified by the lower degradation temperature of CNC(Yang et al., 2017).

4. Conclusion

CNC was extracted from CF by high-shear enzyme-assisted treatment. The chemical properties of cornhusk, CF, and CNC were characterized by FTIR, XRD, and TGA analyses. The effects of enzyme concentration, treatment time, temperature, particle size, and pH were systematically investigated. The CNC obtained via enzymatic treatment exhibited a uniform dispersion in the suspension and a small particle size, implying that CNC can be potentially employed in biocomposites. Additionally, pectin impurities were effectively removed, as CNC presents a network of connected nanofibrils. FTIR analysis indicated that the hemicelluloses and lignin were removed efficiently. Furthermore, XRD analysis revealed that the enzyme treatment did not destroy the cellulose crystal structure of CNC; the typical scattering exhibited by type I cellulose was maintained, but a decrease in the CI of CNC was observed compared to that of CF. The reduction of CNC crystallinity increases the accessibility of CNC, indicating that CNC can be easily blended with other materials. Compared with CF thermal stability of CNC decreased, and char residue is higher. Future research may be included the preparation and characterization of CNC application.

Declarations

Acknowledgements

This work was supported by the Foundation for the Characteristic Discipline of Processing Technology of Plant Foods, China, for the financial assistance, item number (YSTSXK201817), and the Foundation for Basic Scientific Research Funds of Heilongjiang Provincial Universities, for the financial assistance

(135409412), (SPKF202018). We also wish to thank Heilongjiang Provincial Key Laboratory of Corn Deep Processing Theory and Technology.

Conflicts of interest

There are no conflicts of interest to declare.

Author statement

Haiyan Jin: Validation, Investigation, Software, Writing - Review & Editing. Yinghua Tian: Conceptualization, Methodology, Writing- Original draft preparation. Liqian Teng: Data Curation, Writing-Review & Editing. Jiaqi Yang: Investigation, Methodology. Hongyan Wu: Conceptualization, Methodology. Xiaolan Liu: Conceptualization, Writing-Review & Editing.

References

1. Asrofi, M *et al.*, (2018). Isolation of nanocellulose from water hyacinth fiber (whf) produced via digester-sonication and its characterization, Fibers Polym. 19(8) : 1618-1625. http://dx.doi.org/10.1007/s12221-018-7953-1
2. De Carvalho Mendes, C. A *et al.*, (2015). Isolation and characterization of nanocrystalline cellulose from corn husk, Mater. Lett. 148 : 26-29. http://dx.doi.org/10.1016/j.matlet.2015.02.047i
3. Chao Du e*t al.*, (2016). Characteristics and properties of cellulose nanofibers prepared by tempo oxidation of corn husk, BioResources 11(2) : 5276-5284
4. Chen, W e*t al.*, (2011). Isolation and characterization of cellulose nanofibers from four plant cellulose fibers using a chemical-ultrasonic process, Cellulose 18(2) : 433-442. http://dx.doi.org/10.1007/s10570-011-9497-z
5. Chen, Y. W e*t al.*, (2016). Production of new cellulose nanomaterial from red algae marine biomass Gelidium elegans, Carbohydr Polym 151 : 1210-1219. http://dx.doi.org/10.1016/j.carbpol.2016.06.083
6. Chirayil, C. J e*t al.*, (2014). Isolation and characterization of cellulose nanofibrils from Helicteres isora plant, Ind. Crops Prod. 59 : 27-34. http://dx.doi.org/10.1016/j.indcrop.2014.04.020
7. Dai, H e*t al.*, (2018). Utilization of pineapple peel for production of nanocellulose and film application, Cellulose 25(3) : 1743-1756. http://dx.doi.org/10.1007/s10570-018-1671-0
8. Ditzel, F. I e*t al.*, (2017). Nanocrystalline cellulose extracted from pine wood and corncob, Carbohydr Polym 157 : 1577-1585. http://dx.doi.org/10.1016/j.carbpol.2016.11.036
9. Faradilla, R. H. F e*t al.*, (2017). Characteristics of a free-standing film from banana pseudostem nanocellulose generated from TEMPO-mediated oxidation, Carbohydr Polym 174: 1156-1163. http://dx.doi.org/10.1016/j.carbpol.2017.07.025
10. Flauzino Neto, W. P e*t al.*, (2013). Extraction and characterization of cellulose nanocrystals from agro-industrial residue – Soy hulls, I Ind. Crops Prod. 42 : 480-488.

http://dx.doi.org/10.1016/j.indcrop.2012.06.041

11. Haafiz, M. K e*t al.*, (2014). Isolation and characterization of cellulose nanowhiskers from oil palm biomass microcrystalline cellulose, Carbohydr Polym 103 : 119-25. http://dx.doi.org/10.1016/j.carbpol.2013.11.055
12. Hemmati, F e*t al.*, (2018). Synthesis and characterization of cellulose nanocrystals derived from walnut shell agricultural residues, International Int. J. Biol. Macromol 120(Pt A) : 1216-1224. http://dx.doi.org/10.1016/j.ijbiomac.2018.09.012
13. Henriksson, M e*t al.*, (2007). An environmentally friendly method for enzyme-assisted preparation of microfibrillated cellulose (MFC) nanofibers, Eur. Polym. J. 43(8) : 3434-3441. http://dx.doi.org/10.1016/j.eurpolymj.2007.05.038
14. Henrique, M. A e*t al.*, (2013). Valorization of an agro-industrial waste, mango seed, by the extraction and characterization of its cellulose nanocrystals, J. Environ. Manage. 121: 202-9. http://dx.doi.org/10.1016/j.jenvman.2013.02.054
15. Ishikawa, A e*t al.*, (1997). Fine structure and tensile properties of ramie fibres in the crystalline form of cellulose I, II, IIII and IVI, Polymer 38(2) : 463-468. http://dx.doi.org/10.1016/S0032-3861(96)00516-2
16. Islam, M. S e*t al.*, (2011). Influence of alkali fiber treatment and fiber processing on the mechanical properties of hemp/epoxy composites, J. Appl. Polym. Sci. 119(6) : 3696-3707. http://dx.doi.org/10.1002/app.31335
17. Johar, N e*t al.*, (2012). Extraction, preparation and characterization of cellulose fibres and nanocrystals from rice husk, Ind. Crops Prod. 37(1) : 93-99. http://dx.doi.org/10.1016/j.indcrop.2011.12.016
18. Kargarzadeh, H e*t al.*, (2017). Recent developments on nanocellulose reinforced polymer nanocomposites: A review, Polymer 132 : 368-393. http://dx.doi.org/10.1016/j.polymer.2017.09.043
19. Kargarzadeh, H e*t al.*, (2017). Methods for extraction of nanocellulose from various sources, Handbook of nanocellulose and cellulose nanocomposites 1 : 1-51. http://dx.doi.org/10.1002/9783527689972.ch1
20. Khawas, P and Deka, S. C. (2016). Isolation and characterization of cellulose nanofibers from culinary banana peel using high-intensity ultrasonication combined with chemical treatment, Carbohydr Polym 137 : 608-616. http://dx.doi.org/10.1016/j.carbpol.2015.11.020
21. Kumari, P e*t al.*, (2019). Cellulose nanofibers from lignocellulosic biomass of lemongrass using enzymatic hydrolysis: characterization and cytotoxicity assessment, DARU 27(2) : 683-693. http://dx.doi.org/10.1007/s40199-019-00303-1
22. Lagerwall, J. P. F e*t al.*, (2014). Cellulose nanocrystal-based materials: from liquid crystal self-assembly and glass formation to multifunctional thin films, NPG Asia Materials 6(1) : e80-e80. http://dx.doi.org/10.1038/am.2013.69
23. Li, M e*t al.*, (2014). Preparation and characterization of cellulose nanofibers from de-pectinated sugar beet pulp, Carbohydr Polym 102 : 136-43. http://dx.doi.org/10.1016/j.carbpol.2013.11.021

24. Liangbing Hu e*t al.*, (2013). Transparent and conductive paper from nanocellulose fibers, Energy Environ. Sci. 6(2) : 513-518. http://dx.doi.org/10.1039/c2ee23635d
25. Liu, C e*t al.*, (2014). Catalytic fast pyrolysis of lignocellulosic biomass, Chem Soc Rev 43(22) : 7594-623. http://dx.doi.org/10.1039/c3cs60414d
26. Mahardika, M e*t al.*, (2018). Production of nanocellulose from pineapple leaf fibers via high-shear homogenization and ultrasonication, Fibers 6(2) : 28. http://dx.doi.org/10.3390/fib6020028
27. Mandal, A and Chakrabarty, D. (2011). Isolation of nanocellulose from waste sugarcane bagasse (SCB) and its characterization, Carbohydr Polym 86(3) : 1291-1299. http://dx.doi.org/10.1016/j.carbpol.2011.06.030
28. Mohaiyiddin, M. S e*t al.*, (2016). Characterization of nanocellulose recovery from Elaeis guineensis frond for sustainable development, Clean Technol. Environ. Policy 18(8) : 2503-2512. http://dx.doi.org/10.1007/s10098-016-1191-2
29. Natarajan, B e*t al.*, (2018). Binary cellulose nanocrystal blends for bioinspired damage tolerant photonic films, Adv. Funct. Mater. 28(26): 1800032. http://dx.doi.org/10.1002/adfm.201800032
30. Rahbar Shamskar, K e*t al.*, (2016). Preparation and evaluation of nanocrystalline cellulose aerogels from raw cotton and cotton stalk, Ind. Crops Prod. 93 : 203-211.http://dx.doi.org/10.1016/j.indcrop.2016.01.044
31. Reddy, N and Yang, Y. (2005). Properties and potential applications of natural cellulose fibers from cornhusks, Green Chem 7(4) : 190. http://dx.doi.org/10.1039/b415102j
32. Singh, S e*t al.*, (2017). Microwave-assisted step reduced extraction of seaweed (Gelidiella aceroso) cellulose nanocrystals, Int J Biol Macromol 99 : 506-510. http://dx.doi.org/10.1016/j.ijbiomac.2017.03.004
33. Sun, R e*t al.*, (2000). Physico-chemical and structural characterization of hemicelluloses from wheat straw by alkaline peroxide extraction, Polymer 41(7) : 2647-2656. http://dx.doi.org/10.1016/S0032-3861(99)00436-X
34. Suqin Luo , e*t al.*, (2018). Effect of different preparation methods on the structure of pineapple peel nanocellulose, Packaging & food 36(05) : 1-6. http://dx.doi.org/CNKI:SUN:BZSJ.0.2018-05-001
35. Trache, D e*t al.*, (2017). Recent progress in cellulose nanocrystals: sources and production, Nanoscale 9(5): 1763-1786. http://dx.doi.org/10.1039/c6nr09494e
36. Ullah, H e*t al.*, (2016). Advances in biomedical and pharmaceutical applications of functional bacterial cellulose-based nanocomposites, Carbohydr Polym 150 : 330-52. http://dx.doi.org/10.1016/j.carbpol.2016.05.029
37. Wang, H e*t al.*, (2016). Isolating nanocellulose fibrills from bamboo parenchymal cells with high intensity ultrasonication, Holzforschung 70(5) : 401-409. http://dx.doi.org/10.1515/hf-2015-0114
38. Xia Li e*t al.*, (2012). Preparation and characterization of bamboo fiber nanocrystalline cellulose by controlled enzymatic hydrolysis, Proceedings of the 15th Annual Conference of China Paper Society Beijing China, p. 5.

39. Xiao, S e*t al.*, (2016). Poly(vinyl alcohol) films reinforced with nanofibrillated cellulose (NFC) isolated from corn husk by high intensity ultrasonication, Carbohydr Polym 136 : 1027-34. http://dx.doi.org/10.1016/j.carbpol.2015.09.115
40. Yang, X e*t al.*, (2017). Effects of preparation methods on the morphology and properties of nanocellulose (NC) extracted from corn husk, Ind. Crops Prod. 109 : 241-247. http://dx.doi.org/10.1016/j.indcrop.2017.08.032
41. Yang, X e*t al.*, (2017). Impact of dimethyl sulfoxide treatment on morphology and characteristics of nanofibrillated cellulose isolated from corn husks, Bioresources 12(1) : 95-106. http://dx.doi.org/10.15376/biores.12.1.95-106

Figures

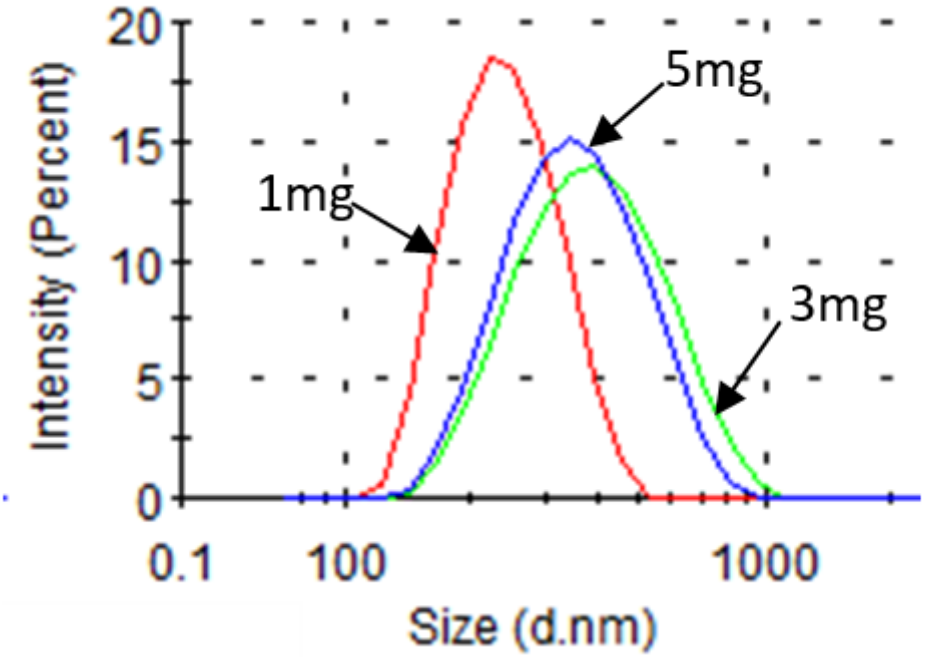

Figure 1

Effect of enzyme concentration on particle size distribution of CNC.

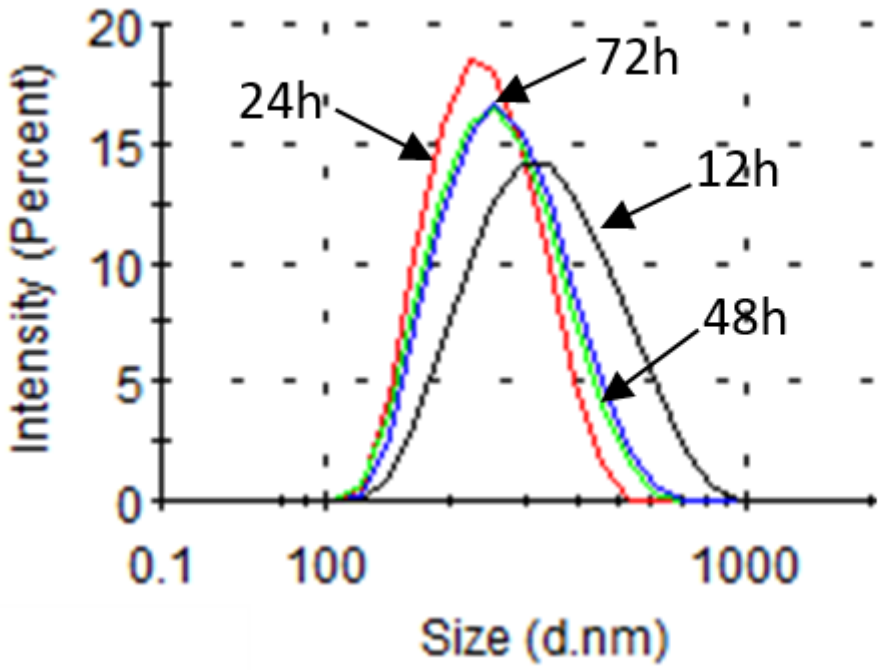

Figure 2

Effect of treatment time on particle size distribution of CNC.

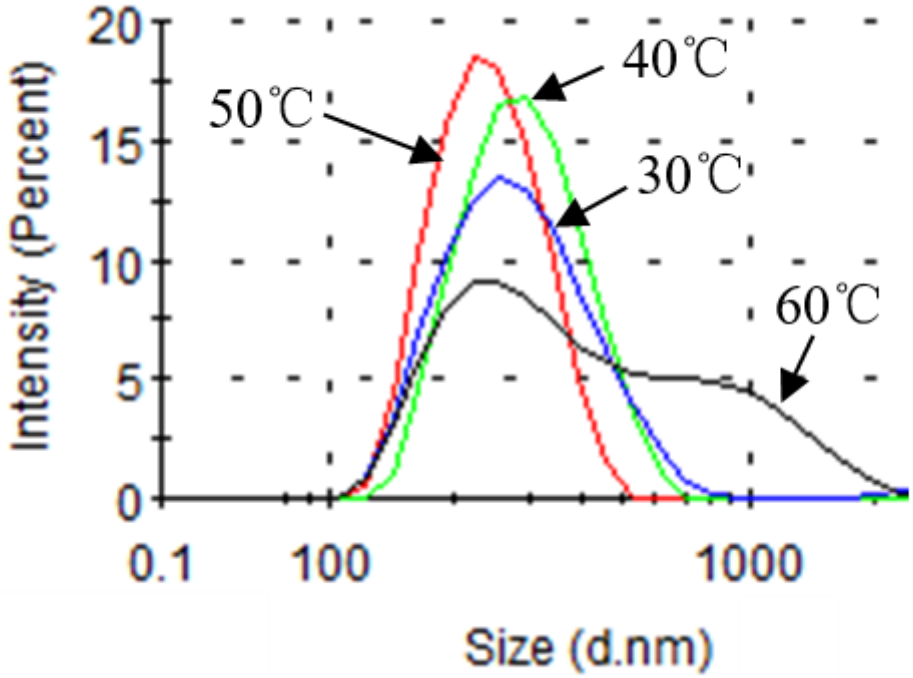

Figure 3

Effect of treatment temperature on particle size distribution of CNC.

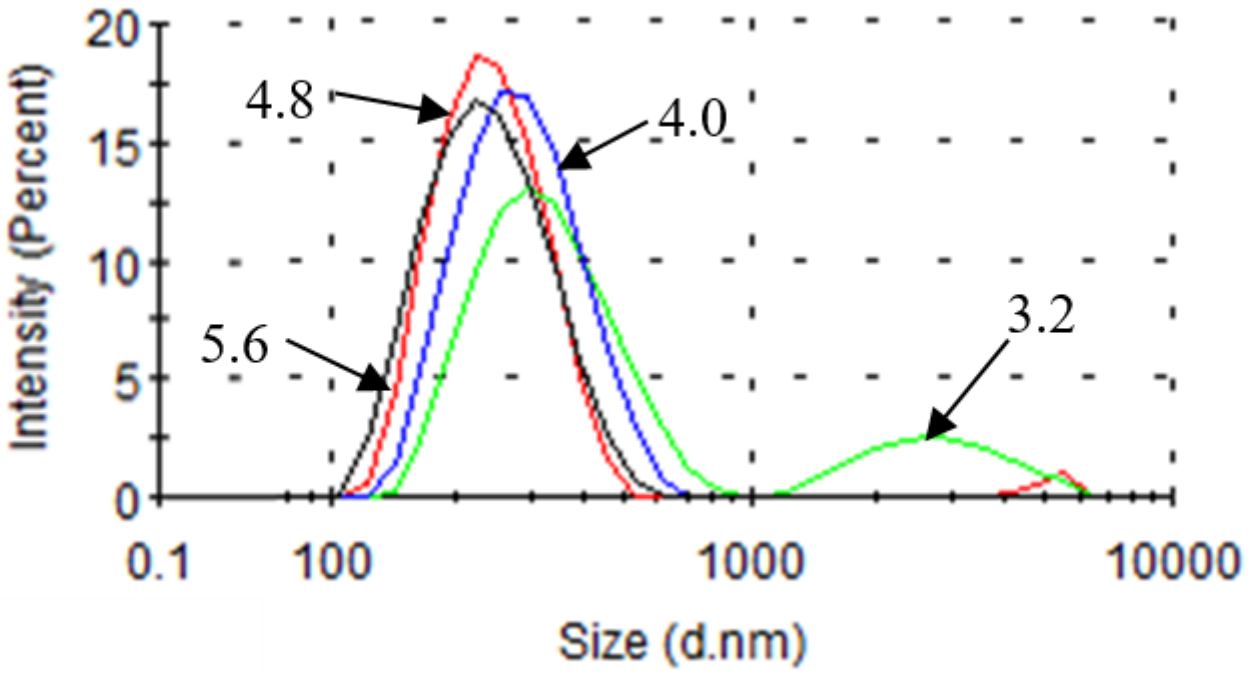

Figure 4

The effect of pH on particle size distribution of CNC.

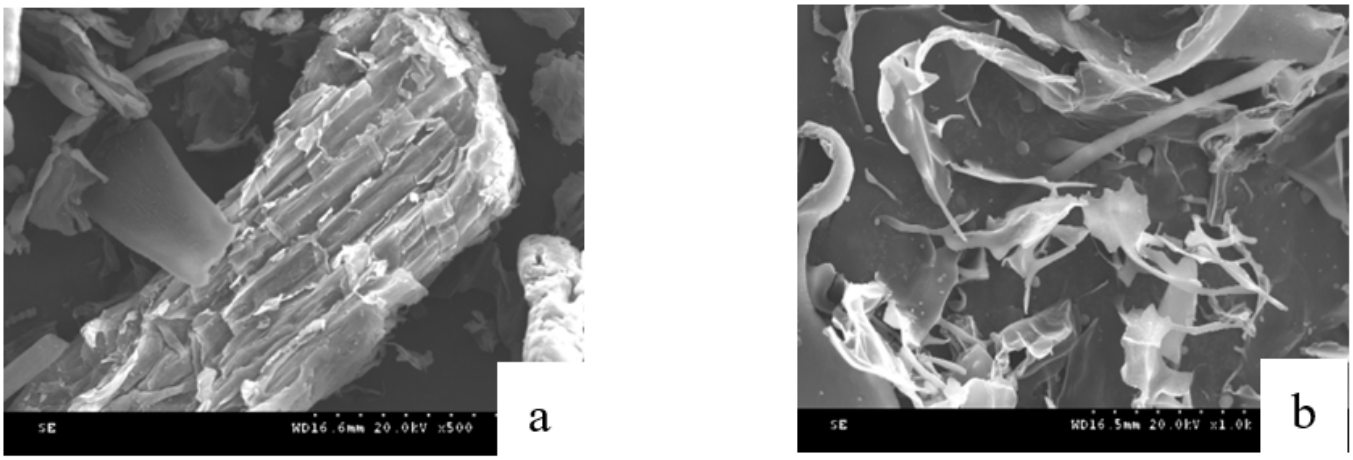

Figure 5

Surface morphology of CF(a) and CNC(b) by SEM.

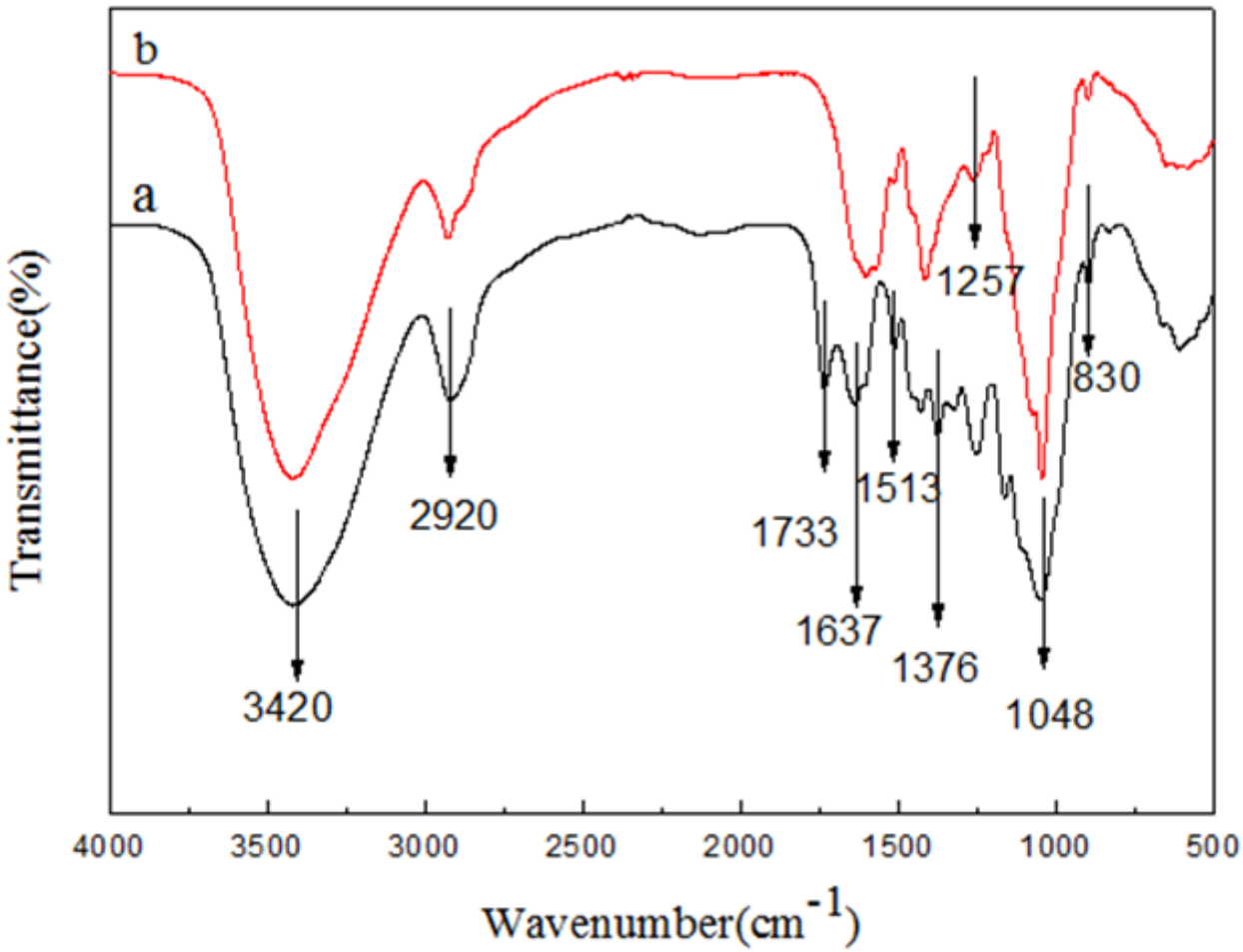

Figure 6

FTIR spectra of CF(a) and CNC(b).

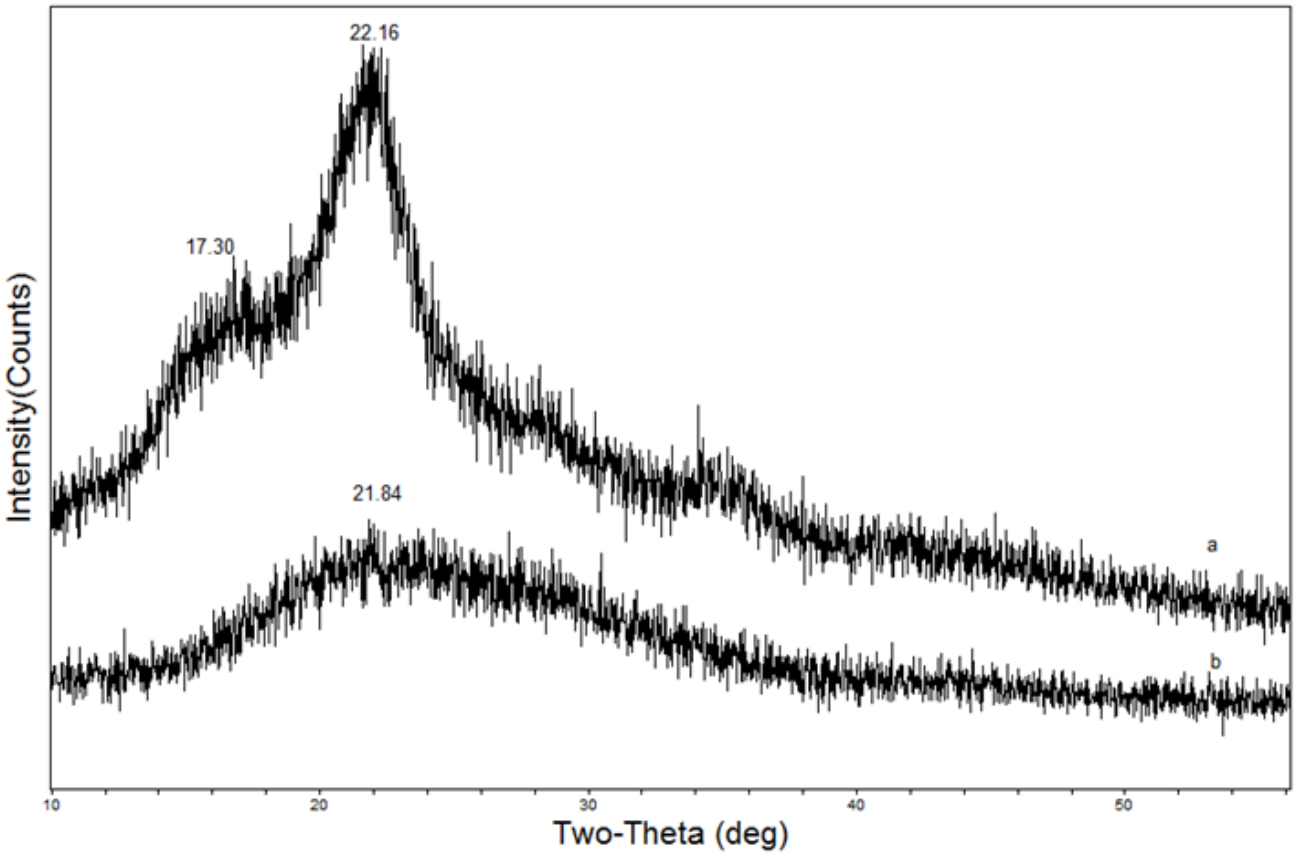

Figure 7

XRD patterns of CF(a) and CNC(b).

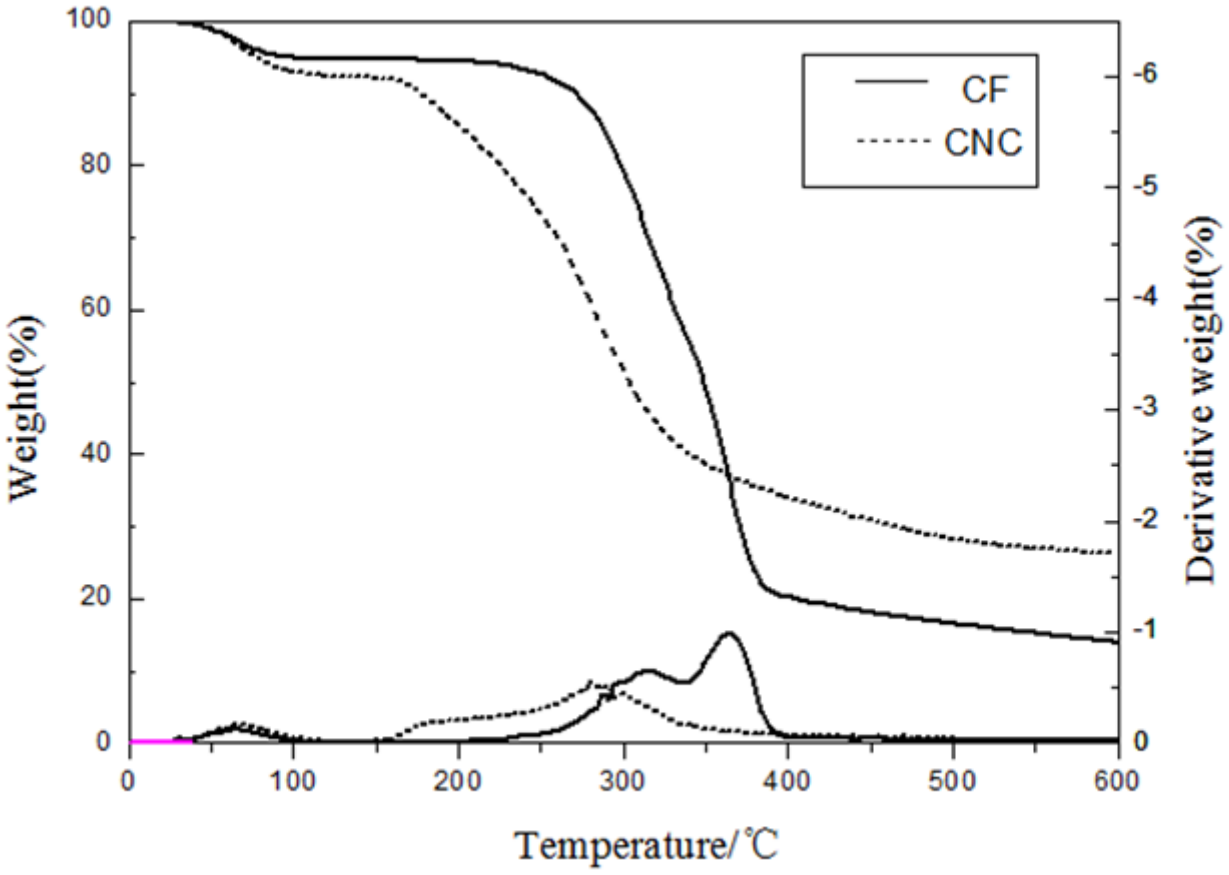

Figure 8

TGA and its derivative thermograms for CF and CNC.

Supplementary Files

This is a list of supplementary files associated with this preprint. Click to download.

- GraphicalAbstracts.pdf